CrossMark

J. Appl. Probab. **59,** 131–151 (2022)
*doi:*10.1017/jpr.2021.34

INTERSECTIONS OF RANDOM SETS

JACOB RICHEY,* *University of British Columbia*
AMITES SARKAR,** *Western Washington University*

Abstract

We consider a variant of a classical coverage process, the Boolean model in $\mathbb{R}^d$. Previous efforts have focused on convergence of the unoccupied region containing the origin to a well-studied limit C. We study the intersection of sets centered at points of a Poisson point process confined to the unit ball. Using a coupling between the intersection model and the original Boolean model, we show that the scaled intersection converges weakly to the same limit C. Along the way, we present some tools for studying statistics of a class of intersection models.

Keywords: Poisson process; random tessellation; Crofton cell

2020 Mathematics Subject Classification: Primary 60D05
Secondary 53C65

1. Introduction

The Boolean model is a geometric model for random sets in space, for example comets striking the moon, or antibodies attaching to a virus. One starts with a Poisson point process $\mathcal{X}$ of intensity λ on $\mathbb{R}^d$ (see Appendix A for some background on Poisson processes), and, for simplicity, some fixed set S. The Boolean model refers to the set $B_{\lambda,S} = \bigcup_{X\in\mathcal{X}} (X + S)$, where, for $x \in \mathbb{R}^d$, $x + S = \{x + y : y \in S\}$. Conditioning on the (positive probability) event $\{0 \notin B_{\lambda,S}\}$, we can then study, among other things, the uncovered component of $\mathbb{R}^d$ containing 0, known as the *Crofton cell*.

The Boolean model was first defined and studied in the 1960s by E. N. Gilbert, who investigated both percolation [12] and coverage [13]. Gilbert's results (from both papers) were improved by Hall [15,16], and Hall's result on coverage [15] was improved and generalized by Janson [19] and Molchanov [26]. The books by Meester and Roy [22] and Hall [17] are standard references for the percolation and coverage processes respectively, and the more recent books by Haenggi [18] and Franceschetti and Meester [11] cover applications to wireless networks (the motivating example from [12]).

There are a number of well-studied cousins of the Boolean model. One such class of models is tessellations. For example, consider a hyperplane tessellation of intensity λ on $\mathbb{R}^d$. Namely, let $\mathcal{R} = \{R_n : n \in \mathbb{N}\}$ denote a Poisson point process with intensity λ (or, more generally, with intensity measure ν) on $\mathbb{R}$, and let θ_n, $n \in \mathbb{N}$, be independent and identically distributed (i.i.d.) uniform over the $(d-1)$-dimensional unit sphere, independent of $\mathcal{R}$. The corresponding Poisson field $\mathcal{H}$ refers to the set of hyperplanes H_n given by $H_n = \{x \in \mathbb{R}^d : x \cdot \theta_n = R_n\}$, i.e. H_n

Received 1 June 2020; revision received 15 April 2021.
* Postal address: 1984 Mathematics Rd, Vancouver BC V6T 1Z2, Canada. Email: jfrichey001@gmail.com
** Postal address: 516 High Street, Bellingham WA 98225, USA. Email: amites.sarkar@wwu.edu

© The Author(s), 2022. Published by Cambridge University Press on behalf of Applied Probability Trust.

https://doi.org/10.1017/jpr.2021.34 Published online by Cambridge University Press

is the hyperplane passing through the point $R_n\theta_n$ with normal vector parallel to θ_n. Note that, on average, 2λ hyperplanes intersect the unit sphere in this model. The analogous object in this context is the connected component of the tessellation containing 0, denoted D_0^λ.

Hyperplane tessellations have a history dating back to the 19th century. Crofton's formula (1868) expresses the length of a curve C in terms of the expected number of times C meets a random line, i.e. the expected number of times C intersects a random line tessellation. Generalizations of Crofton's formula led to the development of integral geometry [29]. Meanwhile, inspired by a question of Niels Böhr on cloud chamber tracks, [14] computed the variance of the cell size in a random line tessellation, and [24,25] initiated the systematic study of random line tessellations (with potential applications to papermaking in mind). We will make use of [14] later. A recent survey article [5] gives an excellent overview of the field.

We will also use a slightly different tessellation model: tessellation by spheres, rather than hyperplanes. Let $\mathcal{X}$ be a Poisson point process of intensity λ on $\mathbb{R}^d$, and let $\mathbb{S} = \partial\mathbb{B} = \{x \in \mathbb{R}^d : ||x||_2 = 1\}$ denote the boundary of the unit ball $\mathbb{B}$ in $\mathbb{R}^d$. Then the set $\bigcup_{X\in\mathcal{X}} (X + \mathbb{S})$ partitions $\mathbb{R}^d$ into a union of disjoint connected components. As before, it is common to study the connected component of this tessellation containing the origin, denoted E_0^λ.

A result from [23] (see also [6]) gives a common scaling limit for these sets.

Theorem 1.1. *Let C_0^λ, D_0^λ, and E_0^λ denote the Crofton cell in the Boolean model (with $S = \mathbb{B}$), and the connected components containing the origin in the hyperplane and sphere tessellation models, respectively. These three models have a common scaling limit in distribution: $\lim_{\lambda\to\infty} S_d\lambda C_0^\lambda \sim \lim_{\lambda\to\infty} 2\lambda D_0^\lambda \sim \lim_{\lambda\to\infty} 2S_d\lambda E_0^\lambda \sim 2C$, where S_d is the surface area measure of $\mathbb{S} = \partial\mathbb{B}$, C is the law of the normalized Crofton cell D_0^1, and $\sim$ denotes equality in distribution.*

The scaling in this theorem is nontrivial and deserves some comment. Consider first the tessellation models. As $\lambda \to \infty$, the expected volume of the connected component containing the origin is inversely proportional to the expected number of connected components in $B_\varepsilon = \{x : ||x|| < \varepsilon\}$. This latter quantity is in turn proportional to the number of points of intersection (of spheres or hyperplanes) in B_ε. The number of such intersection points scales as λ^d, since each intersection point is determined by d spheres (respectively hyperplanes), so the expected volume of the Crofton cell scales as λ^{-d}, leading to a linear scale factor of $1/\lambda$. Finally, the constants can be determined by computing the expected number of spheres (respectively hyperplanes) meeting B_ε in each of the three models; for C_0^λ, D_0^λ, and E_0^λ these are asymptotically $S_d\lambda\varepsilon$, $2\lambda\varepsilon$, and $2S_d\lambda\varepsilon$ respectively.

Our contribution is to introduce a new model to this group, which we term the *Boolean intersection model*. Let $\mathbb{B}$ denote the closed unit ball in $\mathbb{R}^d$, and let $\mathcal{C}_\lambda$ be a Poisson point process with intensity λ on $\mathbb{B}$. (We will focus on the uniform intensity case, and discuss in Section 3 some ideas that apply for general intensity measures). Let

$$I^\lambda = \mathbb{B} \cap \left(\bigcap_{C\in\mathcal{C}_\lambda} (C + \mathbb{B}) \right) \tag{1.1}$$

be the intersection of copies of $\mathbb{B}$ shifted by $C \in \mathcal{C}_\lambda$. By definition, set $I^\lambda = \mathbb{B}$ if $\mathcal{C}_\lambda = \emptyset$. Note that for each λ, I^λ is a convex (connected) set contained in $\mathbb{B}$, containing 0. Our goal will be to show that I^λ shares the same limit as the Boolean and Poisson hyperplane tessellation processes, up to a constant.

https://doi.org/10.1017/jpr.2021.34 Published online by Cambridge University Press

Theorem 1.2. *Let C denote the law of the normalized Crofton cell D_0^1. The following distributional convergence holds:*

$$\lim_{\lambda\to\infty} S_d \lambda I^\lambda \sim 2C. \tag{1.2}$$

Write $|I|$ for the Lebesgue measure of a measurable set $I \subset \mathbb{R}^d$, and $\omega_d = \mathrm{vol}(\mathbb{B}) = \frac{1}{d}S_d$.

Proposition 1.1. *The limiting volume of the intersection is given by*

$$\lim_{\lambda\to\infty} \lambda^d \mathbb{E}|I^\lambda| = \frac{d!\omega_d}{\omega_{d-1}^d}.$$

For example, when $d = 2$, $\lim_{\lambda\to\infty} \lambda^2 \mathbb{E}|I^\lambda| = \frac{\pi}{2}$.

One proof of this fact is via (1.2), and an appeal to classical results on the statistics of the Crofton cell C [14]; we outline the details in Section 6. We give an alternative proof based on general results for the intersection model in Section 3. Similar formulas hold for a more general class of Boolean intersection models, namely where the underlying point process is not uniform, or the balls are exchanged for other compact sets. For simplicity we focus on the case of balls of fixed radius, and comment on generalizations in Section 3.2. Additionally, all these results can be formulated using 'fixed count' versions of these models: that is, instead of using an underlying Poisson process, for each n define I_n as the intersection of n i.i.d. translations of $\mathbb{B}$. This model also shares the Crofton cell D_0^1 as a scaling limit.

1.1. Random variables in the space of closed sets

Our main result, Theorem 1.2, refers to a convergence of random sets. The usual modes of convergence – in law, in probability, and in L^p – are trickier to define for random sets. We follow the approach taken in [6] and most of the existing literature, namely via the Hausdorff metric d_{H} on the space E of closed subsets of $\mathbb{R}^d$. Namely, if X_n and X are defined on the same probability space, we say $X_n \to X$ in probability if, for every $\epsilon > 0$,

$$\mathbb{P}(d_{\mathrm{H}}(X_n, X) > \epsilon) \to 0 \qquad \text{as } n \to \infty. \tag{1.3}$$

Our proof of Theorem 1.2 gives an explicit coupling between the intersection model and the Crofton cell, under which (1.3) holds.

2. Overview of results

Although our main result is Theorem 1.2, we will present two different approaches to its corollary, Proposition 1.1. The first is direct, and appears in Section 3. The second is via Theorem 1.2, and occupies Sections 4, 5, and 6. Below, we summarize each approach in turn.

In Section 3, we first consider a single ball B, whose center lies inside the unit ball $\mathbb{B}$. A simple volume calculation lets us estimate (in Proposition 3.1) the probability that B contains the line segment $[0, r]$ on the positive x-axis. Next, we consider the full model, in which unit balls are centered at points of a Poisson process of intensity λ inside $\mathbb{B}$, forming an intersection I^λ. Write R^λ for the radius of I^λ in the positive x direction (for instance). Proposition 3.1, together with an approximation argument, allows us to show that the suitably scaled radius R^λ converges in distribution to an exponential random variable of mean 1. Finally, Proposition 3.3 relates the expected volume of I^λ to the dth moment of R^λ, completing the calculation of $\mathbb{E}|I^\lambda|$ and proving Proposition 1.1.

https://doi.org/10.1017/jpr.2021.34 Published online by Cambridge University Press

As part of this analysis, we also prove a parallel series of results for a related hyperplane model K^λ, which approximates the ball model I^λ near the origin.

Section 4 contains some probabilistic and geometric lemmas that we will use in Section 5.

In Section 5, we prove Theorem 1.2. The main idea is to couple the intersection model with a sphere tessellation model. With I^λ as above, and J^λ defined as the cell containing the origin in an appropriately scaled sphere tessellation model, we show that, in our coupling, the scaled Hausdorff distance between I^λ and J^λ converges to 0 almost surely as $\lambda \to \infty$. To achieve this, we carry out the following steps:

(i) Show that only points of the Poisson process close to the boundary – namely, within distance $\varepsilon_\lambda = \frac{\log^2 \lambda}{\lambda}$ of $\partial\mathbb{B}$ – contribute to the shape of I^λ (asymptotically almost surely as $\lambda \to \infty$). We use a coupon-collector-type process on $\partial\mathbb{B}$ as a test: if there are points of $\mathcal{C}_\lambda$ close to $\partial\mathbb{B}$ that are 'spread out enough' (in terms of angle), then I^λ must be contained within a small ball at the origin.

(ii) Match spheres close to $\partial\mathbb{B}$ from the intersection model with spheres close to $\partial\mathbb{B}$ from the tessellation model. Since some of the sphere centers in the tessellation model land outside $\mathbb{B}$, while the sphere centers in the intersection model are confined to $\mathbb{B}$, we must match them by shifting. We accordingly identify each point $R\theta$ of the underlying tessellation process (with $R \in (1, 1+\varepsilon_\lambda)$ and $\theta \in \partial\mathbb{B}$) with the point $(R-2)\theta$ in the intersection process. The spheres centered at these two points have almost the same effect on J^λ, except that one makes a 'concave' boundary and the other a 'convex' boundary.

(iii) Show that the error in carrying out Step (ii), in terms of the Hausdorff distance between the suitably scaled sets I^λ and J^λ, is negligible. This involves a careful coupling between the underlying point processes: since we scale everything by a factor of λ, it is necessary to have an error of order $o(\lambda^{-1})$, not just $o(1)$.

Finally, in Section 6, we derive Proposition 1.1 from Theorem 1.2, using the d-dimensional version of Goudsmit's 1945 calculation [14] for the area of the Crofton cell. Although the relevant formulas appear in [21, Chapter 6], our treatment is short and self-contained.

3. Statistics for the intersection model

To warm up, consider the following generic intersection process on $\mathbb{R}$. Let $\mathcal{C}_\lambda$ be a Poisson process with intensity λ on $[-1, 1]$, and define $U = U_\lambda = [-1, 1] \cap \left(\bigcap_{c\in\mathcal{C}_\lambda} c + [-1, 1]\right)$, where $c + [-1, 1] = [c-1, c+1]$ for $c \in \mathbb{R}$, with the convention that $U = [-1, 1]$ if $\mathcal{C}_\lambda = \emptyset$. U is always an interval, so it is determined by $\sup U$ and $\inf U$. The distribution of the infimum can be determined as follows. We have that $\inf U < -u$ if and only if $\max \mathcal{C}_\lambda < 1-u$, which in turn holds if and only if each element of $\mathcal{C}_\lambda$ is less than $1-u$, i.e. if no point of $\mathcal{C}_\lambda$ lies in the interval $[1-u, 1]$. The latter event has probability $e^{-\lambda u}$, so $-\inf U$ is approximately distributed as $\mathrm{Exp}(\lambda^{-1})$ as $\lambda \to \infty$.

Note that $\inf U$ is a function of $\mathcal{C}_\lambda \cap [0, 1]$ and $\sup U$ is a function of $\mathcal{C}_\lambda \cap [-1, 0]$; basic properties of Poisson processes imply that $\inf U$ and $\sup U$ are independent. Thus, as $\lambda \to \infty$, the left and right endpoints of U shrink to 0 independently, and $\lambda|U_\lambda| \to_{\mathrm{d}} \mathrm{Exp}(1) + \mathrm{Exp}(1) \sim \mathrm{Gamma}(2, 1)$.

https://doi.org/10.1017/jpr.2021.34 Published online by Cambridge University Press

3.1. Ball and hyperplane intersection models

We now explore some basic properties of two intersection models: the ball intersection model I^λ, defined as in (1.1), and an analogous intersection model with hyperplanes. Let $\widetilde{\mathcal{C}}_\lambda$ be a Poisson point process on $\mathbb{B}$ with intensity measure $\lambda(\nu \times \sigma)$, where σ is the surface-area measure on $\mathbb{S}$ and ν is the measure, supported on $[0, 1]$, given by $\nu(0, r) = \frac{1}{d}\left(1 - (1-r)^d\right)$. Define the hyperplane intersection model $K^\lambda = \mathbb{B} \cap \left(\bigcap_{\widetilde{C} \in \widetilde{\mathcal{C}}_\lambda} \mathbb{H}(\widetilde{C})\right)$, where $\mathbb{H}(\widetilde{C})$ is the half-space normal to the vector $\widetilde{C}$ and containing 0, i.e. $\mathbb{H}(\widetilde{C}) = \widetilde{C} + \{x \in \mathbb{R}^d : x \cdot \widetilde{C} < 0\}$. By definition, $K^\lambda = \mathbb{B}$ if $\widetilde{\mathcal{C}}_\lambda = \emptyset$. The choice of ν is special, because it makes K^λ asymptotically identical to the Boolean intersection model I^λ with copies of $\mathbb{B}$ defined earlier – the difference is that the copies of the unit disk have been exchanged for half-spaces. Indeed, placing a single disk $\mathbb{B}$ with center $Z\Theta$ is like placing the half-space $\mathbb{H}((Z-1)\Theta)$; the difference is asymptotically negligible as $\lambda \to \infty$. The error is quantified precisely in terms of the Hausdorff distance in Section 4. In this section we work with both K^λ and I^λ simultaneously: the same ideas can be used to analyze both models, with slightly different details.

For any $\theta \in \mathbb{S}$, define the 'radius in the θ direction':

$$R^\lambda(\theta) = \sup\{t \in (0, 1) : t\theta \in I^\lambda\}, \qquad Q^\lambda(\theta) = \sup\{t \in (0, 1) : t\theta \in K^\lambda\}. \tag{3.1}$$

The collections $\{R^\lambda(\theta) : \theta \in \mathbb{S}\}$ and $\{Q^\lambda(\theta) : \theta \in \mathbb{S}\}$ each consist of identically distributed but not independent variables: $R^\lambda(\theta)$ and $R^\lambda(\theta')$ are not independent for $\theta \neq \theta'$ (except for the special case $\theta' = -\theta$). We simply write $R = R^\lambda$ or $Q = Q^\lambda$ for the distribution of any one of the $R^\lambda(\theta)$ or $Q^\lambda(\theta)$, respectively. For $r \in (0, 1)$, denote by $F(r)$ and $G(r)$ the probabilities

$$F(r) = \mathbb{P}(re_1 \notin B), \qquad G(r) = \mathbb{P}(re_1 \notin H), \tag{3.2}$$

in which $B = \mathbb{B} + C$, where C is a uniformly distributed point in $\mathbb{B}$, H is an independent copy of one of the random hyperplanes $\mathbb{H}(\widetilde{C})$, $\widetilde{C} \in \widetilde{\mathcal{C}}_\lambda$, and $\vec{e}_1 = (1, 0, \ldots, 0) \in \mathbb{R}^d$. The functions F and G are closely connected to the distributions of R and Q respectively, since, for $r \in (0, 1)$, $R > r$ if and only if $r\vec{e}_1 \in \mathbb{B} + C$ for every $C \in \mathcal{C}_\lambda$, and similarly for Q. Recall that ω_d denotes the volume of the unit ball $\mathbb{B}$ in $\mathbb{R}^d$. We have the following formulas for F and G.

Proposition 3.1. *Consider the intersection Boolean models I^λ and K^λ in dimension $d \geq 1$.*

(i) *Let F be as in (3.2). For any $r \in (0, 1)$,*

$$F(r) = \frac{1}{\omega_d} |\mathbb{B} \setminus (r\vec{e}_1 + \mathbb{B})| = \frac{\omega_{d-1}}{\omega_d} r - O(r^3) \qquad \text{as } r \to 0,$$

where $|\cdot|$ denotes the volume (Lebesgue measure) in $\mathbb{R}^d$. Moreover, for $r \in [0, 1]$ we have $r \leq CF(r)$ for some constant C depending only on the dimension.

(ii) *Let G be as in (3.2), and write $\mathbb{S}^+ = \{\theta \in \mathbb{S} : \langle \theta, \vec{e}_1 \rangle > 0\}$. For any $r \in (0, 1)$,*

$$\begin{aligned} G(r) &= \frac{1}{\omega_d} \int_{\mathbb{S}^+} \nu(0, r\langle \vec{e}_1, \theta \rangle) \, \mathrm{d}\sigma(\theta) \\ &= \nu \times \sigma \left(\frac{r(\vec{e}_1 + \mathbb{B})}{2} \right) \\ &= \frac{(d-1)\omega_{d-1}}{d\omega_d} \sum_{k=1}^{d} (-1)^{1+k} \binom{d}{k} \frac{\Gamma\left(\frac{d-1}{2}\right)\Gamma\left(\frac{k+1}{2}\right)}{2\Gamma\left(\frac{k+d}{2}\right)} r^k \\ &= \frac{\omega_{d-1}}{\omega_d} r - O(r^2) \qquad \text{as } r \to 0. \end{aligned} \tag{3.3}$$

https://doi.org/10.1017/jpr.2021.34 Published online by Cambridge University Press

Note that F and G have the same linear approximation near 0. This is a reflection of the fact that the unit ball has a smooth boundary, and hence locally is a hyperplane.

Proof. (i) Write $B = C + \mathbb{B}$, where C is uniform over $\mathbb{B}$, and note that, for $r \in (0, 1)$, $r\vec{e_1} \notin B$ if and only if $\|C - r\vec{e_1}\| > 1$, if and only if $C \in \mathbb{B} \setminus (r\vec{e_1} + \mathbb{B})$. The first equality follows immediately. The shape $\text{Lune}(r) = \mathbb{B} \setminus (r\vec{e_1} + \mathbb{B})$ is very close to the shape $\text{Wedge}(r) = \{\theta + t\vec{e_1} : \theta \in \mathbb{S}^-, t \in (0, r)\}$ obtained by shifting half of $\mathbb{S}$ by r along the $\vec{e_1}$ axis, where $\mathbb{S}^- = \{\theta \in \mathbb{S} : \langle \theta, \vec{e_1} \rangle < 0\}$. The volume of $\text{Wedge}(r)$ is $|\text{Wedge}(r)| = \omega_{d-1} r$.

Note that $\text{Lune}(r) = \text{Wedge}(r) \cap \mathbb{B}$. The 'error' set $\text{Wedge}(r) \setminus \text{Lune}(r)$ is contained in a region with triangular cross sections; in dimension $d = 2$, it has the form $\text{Wedge}(r) \setminus \text{Lune}(r) = \{(x, y) \in \mathbb{R}^2 : x \in (0, r), y \in (\sqrt{1 - z^2}, 1)\}$, where $z = \min(x, r - x)$ (see Fig. 1). In arbitrary dimension d, the set $\text{Wedge}(r) \setminus \text{Lune}(r)$ is contained in the region formed by rotating the same region about the e_1 axis (i.e. through the copy of the $(d-2)$-dimensional unit sphere lying in the hyperplane $x^1 = 0$). Using the expansion $\sqrt{1 - s^2} = 1 - \frac{s^2}{2} + O(s^4)$, it follows immediately that $|\text{Wedge}(r) \setminus \text{Lune}(r)| \le (d-1)\omega_{d-1} \frac{r^3}{16} + O(r^5)$, proving both parts of the assertion.

(ii) Write $C = P\Theta$, where $P \in [0, 1]$ is distributed according to ν, and $\Theta \in \mathbb{S}$ is distributed according to σ. The corresponding hyperplane, pinned at C, is given by $H = \mathbb{H}(C) = \{x : \langle x, \Theta \rangle \le P\}$, and thus $\mathbb{P}(r\vec{e_1} \notin H) = \mathbb{P}(P < \langle r\vec{e_1}, \Theta \rangle)$.

The first equality follows immediately by integrating. Moreover,

$$P < r\langle \vec{e_1}, \Theta \rangle \iff \left\| P\Theta - \frac{r}{2}\vec{e_1} \right\| < \frac{r}{2} \iff C = P\Theta \in \frac{r(\vec{e_1} + \mathbb{B})}{2},$$

proving the second equality. To obtain the explicit sum formula, we can evaluate the integral directly by expanding the measure ν as $\nu(0, r) = \frac{1}{d}\left(1 - (1 - r)^d\right) = \frac{1}{d}\sum_{k=1}^{d} (-1)^{1+k} \binom{d}{k} r^k$. Thus, for $d \ge 2$,

$$\begin{aligned} G(r) &= \frac{1}{\omega_d} \int_{\mathbb{S}^+} \nu(0, r\langle \vec{e_1}, \theta \rangle)\, \mathrm{d}\sigma(\theta) \\ &= \frac{(d-1)\omega_{d-1}}{d\omega_d} \int_0^{\pi/2} \int_{\mathbb{S}^{d-1}} \sum_{k=1}^{d} (-1)^{1+k} \binom{d}{k} r^k \cos^k \alpha \sin^{d-2} \alpha \, \mathrm{d}\phi \, \mathrm{d}\alpha \\ &= \frac{(d-1)\omega_{d-1}}{d\omega_d} \sum_{k=1}^{d} (-1)^{1+k} \binom{d}{k} \left(\int_0^{\pi/2} \cos^k \alpha \, \sin^{d-2} \alpha \, \mathrm{d}\alpha \right) r^k. \end{aligned}$$

(This integral is not valid when $d = 1$: in that case, $G(r) = F(r) = 2r$.) The $\mathrm{d}\alpha$ integral evaluates to

$$\int_0^{\pi/2} \cos^k \alpha \, \sin^{d-2} \alpha \, \mathrm{d}\alpha = \frac{\Gamma\left(\frac{d-1}{2}\right)\Gamma\left(\frac{k+1}{2}\right)}{2\Gamma\left(\frac{k+d}{2}\right)},$$

and the coefficient of the linear term ($k = 1$) is

$$\frac{(d-1)\omega_{d-1}}{d\omega_d} \cdot d \cdot \frac{\Gamma\left(\frac{d-1}{2}\right)}{2\Gamma\left(\frac{d+1}{2}\right)} = \frac{\omega_{d-1}}{\omega_d}.$$

□

For example, in dimension $d = 2$, an explicit computation – namely, for the area of intersection of two circles – yields

$$F(r) = 1 - \frac{1}{\pi}\left(2 \arccos(r/2) - r\sqrt{1 - r^2/4}\right) = \frac{2r}{\pi} - \frac{r^3}{12\pi} + \cdots \tag{3.4}$$

https://doi.org/10.1017/jpr.2021.34 Published online by Cambridge University Press

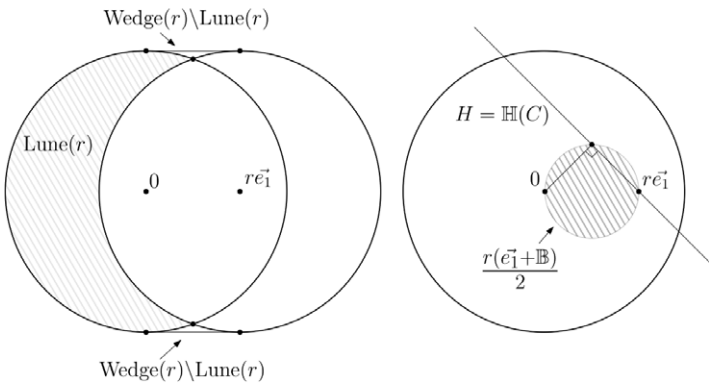


FIGURE 1. The left diagram shows $F(r)$ as the area of the shaded set. Note that if any disk center lies in the lune, then I^λ does not contain the point $(r,0)$. The error between the Lune and Wedge sets is indicated with arrows; its area is negligible, and this gives a quick approximation of the area of the lune. The analogous set for the hyperplane model is shown on the right: $G(r)$ is the mass placed on the shaded set by the probability measure $\frac{1}{S_d}\nu \times \sigma$. The fact that the shaded set is a circle follows from elementary geometry: the angle in a semicircle is a right angle.

Directly evaluating the integral (3.3) gives

$$G(r) = \frac{1}{\pi}\int_0^{\pi/2} (2r\cos\theta - r^2\cos^2\theta)\,\mathrm{d}\theta = \frac{2r}{\pi} - \frac{r^2}{4}.$$

Recall that R and Q depend on d via the underlying dimension of the Boolean intersection models I^λ and K^λ. The distributions of R^λ and Q^λ converge to exponential distributions as $\lambda \to \infty$.

Proposition 3.2. *For any $d \geq 1$, as $\lambda \to \infty$, $\lambda\omega_d F(R^\lambda) \to \mathrm{Exp}(1)$ and $\lambda\omega_d G(Q^\lambda) \to \mathrm{Exp}(1)$, where the convergence is in distribution.*

Proof. For any $r \in (0, 1)$, since I^λ is the intersection of $\mathrm{Poi}(\lambda\omega_d)$ many copies of $\mathbb{B}$, $\mathbb{P}(R > r) = \mathbb{P}(r\vec{e}_1 \in I^\lambda) = \exp(-\lambda\omega_d F(r))$. Similarly, $\mathbb{P}(Q > r) = \exp(-\lambda\omega_d G(r))$. Fix $z \in (0, \lambda\omega_d)$. Note that F and G are strictly increasing on $[0, 1]$, and hence invertible. Thus, we can write

$$\mathbb{P}(\lambda\omega_d F(R) > z) = \mathbb{P}(R > F^{-1}(z/\lambda\omega_d)) = \exp(-\lambda\omega_d F(F^{-1}(z/\lambda\omega_d))) = \exp(-z),$$

and similarly for $G(Q)$. Taking $\lambda \to \infty$ finishes the proof. □

Corollary 3.1. *The exact distributions of $\lambda\omega_d F(R)$ and $\lambda\omega_d G(Q)$ are given by*

$$\mathbb{P}(\lambda\omega_d F(R) > z) = \mathbb{P}(\lambda\omega_d G(Q) > z) = \begin{cases} \mathrm{e}^{-z} & 0 \leq z < \lambda\omega_d, \\ 0 & z > \lambda\omega_d. \end{cases}$$

The collections $\{\lambda F(R)\}_\lambda$ and $\{\lambda G(Q)\}_\lambda$ are uniformly integrable.

Proposition 3.2 leads to a quick calculation for the expected area of I^λ and K^λ via the following proposition, which we state for general random sets. For a continuous function $f : \mathbb{S} \to [0, 1]$, let $U(f) = \{r\theta : r \in [0, f(\theta)], \theta \in \mathbb{S}\}$ be the set with 'radius' $f(\theta)$ in the direction θ.

https://doi.org/10.1017/jpr.2021.34 Published online by Cambridge University Press

Note that, by definition, $I^\lambda = U(R^\lambda)$ and $K^\lambda = U(Q^\lambda)$, where R^λ and Q^λ are viewed as random functions on $\mathbb{S}$ as in (3.1). In general, if $A \subset \mathbb{R}^d$ is closed and star-shaped about the origin, then the function $f_A : \mathbb{S} \to [0, 1]$ given by $f_A(\theta) = \sup\{t \in (0, 1) : t\theta \in A\}$ satisfies $A = U(f_A)$.

A random closed set X is *rotationally invariant* if, for any $\Phi \in \mathrm{SO}(d)$, X has the same distribution as $\Phi(X) = \{\Phi(x) : x \in X\}$.

Proposition 3.3. *Let X be any random closed set contained in $\mathbb{B}$ that is almost surely star-shaped and rotationally invariant. Let $S : \mathbb{S} \to [0, 1]$ be the random function, defined on the same probability space as X, satisfying $X = U(S)$. Then $\mathbb{E}|X| = \omega_d \mathbb{E}\left[S(\vec{e}_1)^d\right]$.*

Proof. The volume of any closed, star-shaped set A with $A = U(f)$, for a continuous function $f : \mathbb{S} \to [0, 1]$, is given by $|A| = \frac{1}{d}\int_{\mathbb{S}} f(\theta)^d \, \mathrm{d}\sigma(\theta)$. (See Appendix B for a proof.) Since X is rotationally invariant, $\mathbb{E}\left[S(\theta)^d\right]$ does not depend on θ. Thus,

$$\begin{aligned}
\mathbb{E}|X| &= \mathbb{E}\left[\frac{1}{d}\int_{\mathbb{S}} S(\theta)^d \, \mathrm{d}\sigma(\theta)\right] \\
&= \frac{1}{d}\int_{\mathbb{S}} \mathbb{E}\left[S(\theta)^d\right] \mathrm{d}\sigma(\theta) \\
&= \frac{1}{d}\int_{\mathbb{S}} \mathbb{E}\left[S(\vec{e}_1)^d\right] \mathrm{d}\sigma(\theta) \\
&= \frac{1}{d}\mathbb{E}\left[S(\vec{e}_1)^d\right] \int_{\mathbb{S}} 1 \, \mathrm{d}\sigma(\theta) \\
&= \omega_d \mathbb{E}\left[S(\vec{e}_1)^d\right].
\end{aligned}$$

Since $X \subset \mathbb{B}$, the expression inside the expectation is almost surely bounded by ω_d, and hence the interchange of integration and expectation is valid by Fubini's theorem. □

Applying this proposition to I^λ and K^λ gives the following corollary.

Corollary 3.2. *For any $d \geq 2$ and $\lambda > 0$, $\mathbb{E}\left|I^\lambda\right| = \omega_d \mathbb{E}(R^\lambda)^d$ and $\mathbb{E}\left|K^\lambda\right| = \omega_d \mathbb{E}(Q^\lambda)^d$.*

We are now ready to compute $\mathbb{E}|I^\lambda|$.

Proposition 3.4. $\lim_{\lambda\to\infty} \lambda^d \mathbb{E}|I^\lambda| = \lim_{\lambda\to\infty} \lambda^d \mathbb{E}|K^\lambda| = \frac{d!\omega_d}{\omega_{d-1}^d}$.

Proof. Here we carry out the details only for I; the analysis for K is similar. We aim to show that $F(R^\lambda)$ is approximately equal to its linear term when λ is large. Let $c > 0$ be any constant. By Proposition 3.2 and the definition of F,

$$\begin{aligned}
\mathbb{P}(R^\lambda > c\lambda^{-1/2}) &= \mathbb{P}(c\lambda^{-1/2}\vec{e}_1 \in I^\lambda) \\
&= \exp\left(-\lambda\omega_d F(c\lambda^{-1/2})\right) \\
&\leq \exp\left(-\lambda\omega_{d-1}(c\lambda^{-1/2} - O(\lambda^{-3/2}))\right) \\
&= \exp\left(-O(\sqrt{\lambda})\right).
\end{aligned}$$

Proposition 3.1 now implies that for some constant $C > 0$,

$$\mathbb{P}\left(\left|F(R^\lambda) - \frac{\omega_{d-1}}{\omega_d} R^\lambda\right| \geq C\lambda^{-3/2}\right) \to 0. \tag{3.5}$$

https://doi.org/10.1017/jpr.2021.34 Published online by Cambridge University Press

Consequently, for any $\varepsilon > 0$,

$$\mathbb{P}\left(\left|\lambda F(R^\lambda) - \lambda\frac{\omega_{d-1}}{\omega_d}R^\lambda\right| \geq \varepsilon\right) \to 0.$$

Since convergence in probability implies convergence in distribution, Proposition 3.2 gives us that $\lambda\omega_d\frac{\omega_{d-1}}{\omega_d}R^\lambda \to_{\mathrm{d}} \mathrm{Exp}(1)$ as $\lambda \to \infty$. By Corollary 3.1, the collection $\{\lambda F(R^\lambda)\}_{\lambda>0}$ is uniformly integrable. By Proposition 3.1, for $r \in [0, 1]$ we have $r \leq CF(r)$ for some constant C depending only on the dimension. Since $R^\lambda \leq 1$ deterministically, it follows that $R^\lambda \leq C \cdot F(R^\lambda)$ for all λ. Thus, the collection $\{\lambda R^\lambda\}_{\lambda>0}$ is also uniformly integrable. Together, convergence in distribution and uniform integrability imply convergence of moments (see [2, Theorem 25.12], for example). Thus, as $\lambda \to \infty$,

$$\lambda^d\mathbb{E}(R^\lambda)^d \to \left(\omega_d \cdot \frac{\omega_{d-1}}{\omega_d}\right)^{-d}\mathbb{E}\big[\mathrm{Exp}(1)^d\big] = \frac{d!}{\omega_{d-1}^d}.$$

Combining this with Proposition 3.3 yields the result. □

3.2. Formulas for general intensity measures

We now give a generalization of these ideas for a wider class of intersection models, where the underlying Poisson process has arbitrary intensity measure, and the sets comprising the intersection are arbitrary. There are many possible ways to generalize this model; we chose a way that yields examples with the same flavor as I^λ and K^λ, but with potentially different asymptotic behavior.

Consider a general Poisson point process $\mathcal{C}_{\mu,\lambda}$ on $[0, 1] \times \mathbb{S}$ with intensity measure $\lambda(\mu \times \sigma)$, where $\lambda > 0$, σ is the surface-area measure on $\mathbb{S}$, and μ is a probability measure on $[0, 1]$. For each $x \in \mathbb{B}$, $x \neq 0$, let $\mathrm{SO}_x(d)$ denote the coset of the subgroup $\mathrm{SO}_{\vec{e}_1}(d)$ of $\mathrm{SO}(d)$ given by $\mathrm{SO}_x(d) = \left\{\Phi \in \mathrm{SO}(d) : \Phi(\vec{e}_1) = \frac{x}{\|x\|}\right\}$. Let $A \subset \mathbb{R}^d$ be a fixed closed convex set such that $\mathbb{B} \subset A$ and $\partial A \cap \partial\mathbb{B} \neq \emptyset$. This assumption ensures that the intersection model almost surely (i) is non-empty for every $\lambda > 0$ and (ii) converges to the set $\{0\}$ as $\lambda \to \infty$.

Note that $\mathrm{SO}_{\vec{e}_1}(d)$ is a compact group, and hence $\mathrm{SO}_x(d)$ has a unique Haar probability measure κ_x. For each $C \in \mathcal{C}_{\mu,\lambda}$, sample a random element $\Phi_C \in \mathrm{SO}_C(d)$ from κ_C. The generalized intersection model $I_A^{\mu,\lambda}$ is $I_A^{\mu,\lambda} = \mathbb{B} \cap \left(\bigcap_{C\in\mathcal{C}_{\mu,\lambda}} \Phi_C(A) + C\right)$. In words, $\Phi_C(A)$ is a copy of A that we give a random spin and pin at a random point; $I_A^{\mu,\lambda}$ is the intersection of a Poisson number of such independent copies. Clearly, $I_A^{\mu,\lambda}$ is rotationally invariant in distribution.

Let ρ and $\widehat{\nu}$ denote the probability measures $\rho(0, r) = r^d$ and $\widehat{\nu}(0, r) = 1 - (1 - r)^d$ for $r \in (0, 1)$. The Boolean intersection models I^λ and K^λ are special cases of the general intersection model with respect to these measures, i.e. $I^\lambda = I_{\mathbb{B}}^{\rho,\lambda}$, $K^\lambda = I_{\mathbb{H}}^{\widehat{\nu},\lambda}$, where $\mathbb{H} = \{x \in \mathbb{R}^d : x \cdot \vec{e}_1 < 1\}$. Define the auxiliary function F_A^μ analogous to F in (3.2): let $A^\mu = \Phi_C(A) + C$ be one of the randomly rotated and shifted copies of A comprising the intersection model $I_A^{\mu,\lambda}$ where C is drawn from the probability measure $\frac{1}{d\omega_d}\mu \times \sigma$, and let $F_A^\mu(r) = \mathbb{P}(r\vec{e}_1 \notin A^\mu)$. There is a simple generic formula in terms of F_A^μ for the expected volume of the intersection.

Fact 3.1. *For any* $\lambda > 0$, $\mathbb{E}\left|I_A^{\mu,\lambda}\right| = d\omega_d \int_0^\infty r^{d-1} \exp\left(-\lambda\omega_d F_A^\mu(r)\right) \mathrm{d}r$.

The proof of Fact 3.1 is a straightforward consequence of a well-known formula for the volume of a random set (see, for example, [27]).

https://doi.org/10.1017/jpr.2021.34 Published online by Cambridge University Press

Proof. Write $I = I_A^{\mu,\lambda}$. By Tonelli's theorem,

$$\begin{aligned}
\mathbb{E}|I| &= \mathbb{E}\int_{\mathbb{R}^d} \mathbf{1}\{x \in I\}\,\mathrm{d}x \\
&= \int_{\mathbb{R}^d} \mathbb{P}(x \in I)\,\mathrm{d}x \\
&= \int_{\mathbb{R}^d} \exp\big(-\lambda\omega_d F_A^{\mu}(||x||)\big)\,\mathrm{d}x \\
&= \int_{\mathbb{S}}\int_0^1 \exp\big(-\lambda\omega_d F_A^{\mu}(r)\big) r^{d-1}\,\mathrm{d}r\,\mathrm{d}\sigma(\theta) \\
&= d\omega_d \int_0^1 r^{d-1}\exp\big(-\lambda\omega_d F_A^{\mu}(r)\big)\,\mathrm{d}r,
\end{aligned}$$

as desired. □

For example, in dimension 2, using the exact equality (3.4) and Fact 3.1 gives the exact formula

$$\mathbb{E}\big|I^{\lambda}\big| = \mathbb{E}\big|I_{\mathbb{B}}^{\rho,\lambda}\big| = 2\pi\int_0^1 r\exp\left(-\lambda + \frac{\lambda}{\pi}\left(2\arccos\left(\frac{r}{2}\right) - r\sqrt{1-\frac{r^2}{4}}\right)\right)\mathrm{d}r.$$

Unfortunately, this integral does not admit a simple asymptotic expansion in λ. The methods of Proposition 3.3, on the other hand, do allow an easy and explicit calculation.

Continuing with the ideas of the previous section, define the radius of the intersection as in (3.1): $I_A^{\mu,\lambda} = \sup\{t \in (0,1) : t\theta \in I^{\mu,\lambda}\}$. The analog of Proposition 3.2 holds in general.

Proposition 3.5. *Let $A \subset \mathbb{R}^d$ be a fixed closed convex set such that $\mathbb{B} \subset A$ and $\partial A \cap \partial\mathbb{B} \neq \emptyset$, and let μ be any probability measure on [0, 1]. As $\lambda \to \infty$, $\lambda\omega_d \cdot F_A^{\mu}(R_A^{\mu,\lambda}) \to_d \mathrm{Exp}(1)$.*

The proof is similar to that of Proposition 3.2. Combining Propositions 3.3 and 3.5 and mimicking the ideas of Proposition 3.4 gives a general program to compute the asymptotic scaling of the volume of $I_A^{\mu,\lambda}$. Below are two examples of intersection models that can be analyzed using this program.

Example 3.1. Consider $I_{\mathbb{H}}^{\rho,\lambda}$ in dimension $d = 2$, i.e. the hyperplane intersection model K^{λ}, but where the underlying Poisson point process is uniform. In this case, $F_{\mathbb{H}}^{\rho}(r) = \int_0^{\pi/2} r^2\cos^2\theta\,\mathrm{d}\theta = \frac{\pi r^2}{4}$. By Proposition 3.5, $\frac{\pi^2}{4}\lambda\cdot\big(R_{\mathbb{H}}^{\rho,\lambda}\big)^2 \to \mathrm{Exp}(1)$. Thus, by Proposition 3.3, $\lambda\mathbb{E}|I_{\mathbb{H}}^{\rho,\lambda}| = \pi\lambda\mathbb{E}(R_{\mathbb{H}}^{\rho,\lambda})^2 \to \pi\cdot\frac{4}{\pi^2} = \frac{4}{\pi}$. Note the difference in scale: $R_{\mathbb{H}}^{\rho,\lambda}$ is roughly $\lambda^{-1/2}$, while $Q^{\lambda} = R_{\mathbb{H}}^{\widehat{\nu},\lambda}$ is roughly λ^{-1}. This limit scaling reflects the behavior of the densities of ρ and $\widehat{\nu}$ near 0.

Example 3.2. Fix $\beta \in (0,\pi)$, and define the cone set

$$\mathrm{Cone}(\vec{e}_1,\beta) = \left\{x \in \mathbb{R}^d : \arccos\left(\frac{\langle x,\vec{e}_1\rangle}{\|x\|}\right) < \beta\right\}.$$

https://doi.org/10.1017/jpr.2021.34 Published online by Cambridge University Press

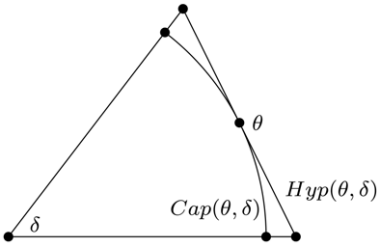


FIGURE 2. The sets Cap(x, y) and Hyp(x, y).

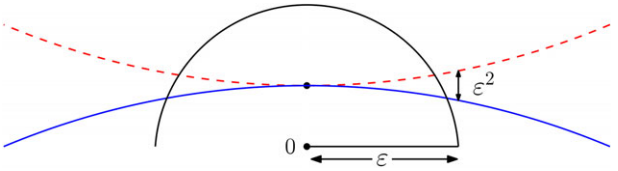


FIGURE 3. On the event that the intersection model is contained in $\mathbb{B}_\varepsilon$, the difference between $(I^\lambda)'$ and J^λ is that some of the copies of $\mathbb{B}$ in the former comprise a concave piece of the boundary (dashed), while those in the latter form a convex boundary piece (solid). The difference is small in Hausdorff distance, because the boundary of the ball is differentiable.

In dimension $d = 2$, we can show that $F^{\rho}_{\mathrm{Cone}(\vec{e}_1,\beta)}(r) \approx C(\beta)r$ as $r \to 0$ for some constant $C(\beta)$, and thus Propositions 3.5 and 3.3 suggest that

$$\mathbb{E}\left|I^{\rho,\lambda}_{\mathrm{Cone}(\vec{e}_1,\beta)}\right| \approx \frac{2}{\pi C(\beta)^2}\lambda^{-2}.$$

Unlike the ball and hyperplane models, however, the cone model does not have the Crofton cell D^1_0 as a scaling limit; see Section 7 for further discussion.

4. Some geometric and probabilistic lemmas

In this section we state some basic lemmas needed to prove Theorem 1.2 via the coupling outlined in Section 2. We begin with some notation. For any $\theta \in \mathbb{S}$, let $\mathrm{Cone}(\theta, \delta)$ denote the cone set

$$\mathrm{Cone}(\theta, \delta) = \left\{x \in \mathbb{R}^d : \arccos\left(\frac{\langle x, \theta\rangle}{\|x\|}\right) < \delta\right\}.$$

Consider the spherical and planar 'caps' $\mathrm{Cap}(\theta, \delta) = \mathrm{Cone}(\theta, \delta) \cap \partial\mathbb{B}$ and $\mathrm{Hyp}(\theta, \delta) = \mathrm{Cone}(\theta, \delta) \cap \{x : x \cdot \theta = 1\}$ (see Fig. 2). Write d_{H} for the Hausdorff distance, defined by $d_{\mathrm{H}}(X, Y) = \max\left\{\sup_{x\in X}\inf_{y\in Y}||x-y||, \sup_{y\in Y}\inf_{x\in X}||x-y||\right\}$. The first fact describes the boundary of the unit ball $\mathbb{B}$.

Fact 4.1. *For δ sufficiently small, $d_{\mathrm{H}}(\mathrm{Cap}(\theta, \delta), \mathrm{Hyp}(\theta, \delta)) = 1 - \cos\delta \le \delta^2$.*

Write $\mathrm{Sh}^-(\varepsilon)$ for the (inner) spherical shell $\mathrm{Sh}^-(\varepsilon) = \{x \in \mathbb{R}^d : ||x|| \in (1-\varepsilon, 1)\}$. Similarly, write $\mathrm{Sh}^+(\varepsilon)$ for the outer spherical shell $\mathrm{Sh}^-(\varepsilon) = \{x \in \mathbb{R}^d : ||x|| \in (1, 1+\varepsilon)\}$, and set $\mathrm{Sh}(\varepsilon) = \mathrm{Sh}^-(\varepsilon) \cup \partial\mathbb{B} \cup \mathrm{Sh}^+(\varepsilon)$.

https://doi.org/10.1017/jpr.2021.34 Published online by Cambridge University Press

Fact 4.2. *For any $\varepsilon > 0$ there is a partition of $\mathrm{Sh}^-(\varepsilon)$ into $K = K(d)$ sets $A_i = A_i(\varepsilon)$, $i = 1, \ldots, K$, such that for any K points $x_i \in A_i$, $i = 1, \ldots, K$, the component of the origin in the Boolean tessellation generated by copies of $\partial\mathbb{B}$ centered at the points x_i is contained in $\mathbb{B}_{2\varepsilon} = \{x : ||x|| < 2\varepsilon\}$, where K does not depend on ε.*

For instance, when $d = 2$, we may take $K(2) = 6$, and make the A_i consecutive thickened arcs of length $\pi/3$. To see this, assume for simplicity that all the points x_i lie on the inner boundary of $\mathrm{Sh}^-(\varepsilon)$, i.e. that $||x_i|| = 1 - \varepsilon$. Then, with $K(2) = 6$, the angle between two consecutive x_i, x_j is at most $2\pi/3$, so that the circles $C_i = x_i + \partial\mathbb{B}$ and $C_j = x_j + \partial\mathbb{B}$ are both tangent to $C_\varepsilon = \partial\mathbb{B}_\varepsilon = \{x : ||x|| = \varepsilon\}$ at points p_i, p_j on C_ε separated by an angle of less than $2\pi/3$. Replacing C_i, C_j by lines l_i, l_j tangent to C_ε at p_i, p_j, we see that l_i and l_j make an angle of at least $\pi/3$ enclosing C_ε, so that their intersection lies in $\mathbb{B}_{2\varepsilon}$; the same applies to the intersection of C_i and C_j.

In higher dimensions, a similar argument applies. Once again, we may assume that the points x_i all satisfy $||x_i|| = 1 - \varepsilon$. The A_i will be thickened cap-like sets partitioning $\mathrm{Sh}^-(\varepsilon)$ in such a way that the angle $x_i O x_i'$ formed by two points $x_i, x_i' \in A_i$ and the origin O is small. Consequently, the corresponding angle formed by points x_i, x_j in adjacent caps A_i, A_j is also small. The spheres $S_i = x_i + \partial\mathbb{B}$ and $S_j = x_j + \partial\mathbb{B}$ are tangent to $S_\varepsilon = \partial\mathbb{B}_\varepsilon = \{x : ||x|| = \varepsilon\}$ at points p_i, p_j as before; we replace S_i, S_j by hyperplanes Π_i, Π_j, tangent to S_ε at p_i, p_j, whose unit normal vectors n_i, n_j are such that $n_i \cdot n_j$ is small. This applies to points in every pair of adjacent caps A_i, A_j, so that the vertices of the polytope formed from the hyperplanes Π_i all lie inside $\mathbb{B}_{2\varepsilon}$.

Upper bounds on $K(d)$ can be obtained from classical results on covering the surface of a high-dimensional unit ball with small spherical caps; see, for instance, [3, Theorem 6.3.1].

We will also need three standard statistical estimates: one regarding the coupon collector process, and two related to Poisson random variables. The 'coupon collector' refers to the following discrete-time process. Given a finite collection of coupons, say $\{1, 2, \ldots, K\} = [K]$, we generate an i.i.d. sequence $(X_t)_{t \le T}$ of $[K]$-valued random variables from any discrete distribution (not necessarily uniform). The process concludes at the stopping time T when every coupon has been collected at least once: $T = \inf\{t \in \mathbb{N} : [K] \subset \{X_1, X_2, \ldots, X_t\}\}$. Very precise results about the distribution of T are known; see, for instance, [9]. Here, we use a simple bound that is convenient for our purposes.

Fact 4.3. *Consider any coupon collector process on K coupons, for $K = K(d)$ as in Fact 4.2. Let T denote the time it takes to collect all K coupons, and let a_* denote the minimum probability of selecting any of the coupons. Then, for any $\lambda > 0$,*

$$\mathbb{P}(T > \log \lambda) < K\lambda^{\log(1-a_*)}. \tag{4.1}$$

We will apply Fact 4.3 in the following way: we collect coupon i when a point of a Poisson process lands in a region A_i. Note that, since the sets A_i appearing in Fact 4.2 do not necessarily have equal volume, the coupon collector process considered in Fact 4.3 is not necessarily uniform. In any case, we can construct the A_i so that $a_* > 0$, and thus the probability in (4.1) goes to 0 as $\lambda \to \infty$.

Proof of Fact 4.3. Let $a_1, a_2, \ldots, a_K$ denote the probabilities of selecting the K coupons respectively, and $a_* = \min\{a_1, a_2, \ldots, a_K\}$. Let $V_i(t)$ denote the indicator random variable of

https://doi.org/10.1017/jpr.2021.34 Published online by Cambridge University Press

the event that coupon i has not been collected by time t, i.e. $V_i(t) = \mathbf{1}_{\{i \notin \{X_1, X_2, \ldots, X_t\}\}}$. Note that $\mathbb{E}V_i(t) = (1 - a_i)^t$. By Markov's inequality,

$$\mathbb{P}(T > t) = \mathbb{P}\left(\sum_{i=1}^{K} V_i(t) \geq 1\right) \leq \sum_{i=1}^{K} \mathbb{E}V_i(t) = \sum_{i=1}^{K} (1 - a_i)^t \leq K(1 - a_*)^t.$$

Setting $t = \log \lambda$ yields the result. □

Proposition 4.1. *Fix any $\mu, \delta > 0$, and let $N \sim \mathrm{Poi}(\mu)$, $N' \sim \mathrm{Poi}(\mu + \delta)$. Then $\mathrm{TV}(N, N') \leq \delta$, where TV denotes total variation distance between probability distributions.*

See, for instance, [1].

Fact 4.4. *Let $Y \sim \mathrm{Poi}(V_\varepsilon \lambda)$, where V_ε is the volume of $Sh(\varepsilon_\lambda)$, and $\varepsilon_\lambda = \lambda^{-1} \log^2 \lambda$. Then $\mathbb{P}(Y < \log \lambda) < \lambda^{-1}$, for sufficiently large λ.*

See [8], for example.

5. Coupling the intersection and tessellation models

The goal of this section is to prove our main convergence result, Theorem 1.2. We carry out the argument for the intersection model with balls, by coupling it to the tessellation model with spheres. Under this coupling, the Hausdorff distance between the two models tends to 0 as $\lambda \to \infty$, even after rescaling both sets by λ.

The coupling works as follows. Let $\mathcal{X} = \mathcal{X}_\lambda$ be a Poisson point process in $\mathbb{R}^d$ of intensity $\frac{\lambda}{2}$, and consider the set $\bigcup_{x \in \mathcal{X}} (x + \partial\mathbb{B})$. Let J^λ be the connected component of the origin in the resulting tessellation. Also, let I^λ denote the ball intersection model on $\mathbb{B}$, i.e. $I^\lambda = \bigcap_{C \in \mathcal{C}_\lambda} (C + \mathbb{B})$, where $\mathcal{C}_\lambda$ is a Poisson point process on $\mathbb{B}$ of intensity λ. The reason that I^λ comes from a point process of intensity twice that of J^λ is that only points inside $\mathbb{B}$ contribute to I^λ, while points both inside and outside $\mathbb{B}$ will contribute to the shape of J^λ. Recalling notation from the previous section, define $\mathcal{X}^\varepsilon = \mathcal{X} \cap \mathrm{Sh}(\varepsilon)$, and consider the 'restricted' model J^λ_ε, the connected component of the origin in the tessellation induced by

$$\bigcup_{x \in \mathcal{X}^\varepsilon} (x + \partial\mathbb{B}). \tag{5.1}$$

Also, let $\mathcal{C}^\varepsilon_\lambda = C_\lambda \cap \mathrm{Sh}(\varepsilon) = C_\lambda \cap \mathrm{Sh}^-(\varepsilon) = \{C \in \mathcal{C}_\lambda : ||C|| \in (1 - \varepsilon, 1)\}$, and define $I^\lambda_\varepsilon = \bigcap_{C \in \mathcal{C}^\varepsilon_\lambda} (C_i + \mathbb{B})$. For ε chosen appropriately, the restricted models are not far from the original models. To be precise, we have the following proposition.

Proposition 5.1. *Set $\varepsilon = \varepsilon_\lambda = \frac{\log^2 \lambda}{\lambda}$. As $\lambda \to \infty$, $\mathbb{P}(J^\lambda_{2\varepsilon} = J^\lambda) \to 1$ and $\mathbb{P}(I^\lambda_{2\varepsilon} = I^\lambda) \to 1$. Moreover, with probability tending to 1, $J^\lambda \subset \mathbb{B}_{2\varepsilon}$ and $I^\lambda \subset \mathbb{B}_{2\varepsilon}$.*

This is essentially the statement that only points near $\partial\mathbb{B}$ contribute to the component of the origin.

Proof. We will prove the assertion for J^λ; the proof for I^λ is similar. The main ingredients are Facts 4.2 and 4.3. Fix any $\lambda > 0$, and let $\{A_i(\varepsilon_\lambda)\}_{i=1}^K$ denote the sets given by Fact 4.2. Consider the stopping time $\lambda^{\mathrm{cov}} = \min\{\eta : \mathcal{X}_\eta \cap A_i(\varepsilon_\lambda) \neq \emptyset \text{ for } i = 1, 2, \ldots, K\}$. We regard the Poisson point processes $\mathcal{X} = \mathcal{X}_\eta$ as nested, i.e. they are coupled so as to form a non-decreasing sequence of sets as η increases. This makes λ^{cov} a well-defined stopping time.

https://doi.org/10.1017/jpr.2021.34 Published online by Cambridge University Press

Fix $\eta > \lambda^{\text{cov}}$. By Fact 4.2, $J^\eta \subset \mathbb{B}_{2\varepsilon_\lambda}$. It follows that any point $y \in \mathcal{X}_\eta \cap \text{Sh}(2\varepsilon_\lambda)^c$ does not contribute to J^η, i.e. $y + \partial\mathbb{B}$ does not lie on the boundary of J^η. Thus, $J^\eta_{2\varepsilon_\lambda} = J^\eta$ in this case.

To finish the proof, it suffices to show that $\mathbb{P}(\lambda^{\text{cov}} < \lambda) \to 1$ as $\lambda \to \infty$. For the above event to occur, the point process $\mathcal{X}_\lambda$ must have at least one point in each set $A_i(\varepsilon_\lambda)$. It is enough to have $\log\lambda$ points of $\mathcal{X}_\lambda$ in $\mathcal{X}^\varepsilon_\lambda$; then, by Fact 4.3, each A_i will have at least one point with high probability. The number of such points is Poisson with mean $V_\varepsilon \cdot \lambda$. By Fact 4.4 and a union bound, and noting that $a_* > 0$,

$$\mathbb{P}(\lambda^{\text{cov}} \geq \lambda) \leq K\lambda^{\log(1-a_*)} + \lambda^{-1} \to 0 \text{ as } \lambda \to \infty. \qquad \square$$

Additionally, the two restricted models are close to each other.

Proposition 5.2. *The random sets I^λ, I^λ_ε, J^λ, and J^λ_ε can be constructed on the same probability space such that as $\lambda \to \infty$, with $\varepsilon = \varepsilon_\lambda/2 = \frac{\log^2\lambda}{2\lambda}$ as in Proposition 5.1, $\mathbb{P}(d_{\text{H}}(\lambda I^\lambda_\varepsilon, \lambda J^\lambda_\varepsilon) \leq C\lambda^{-1/4}) \to 1$, for some global constant $C > 0$.*

Proof. We will give an explicit coupling of the intersection and tessellation models on the same probability space where the two models agree with high probability. The coupling works as follows. We will build the intersection model from the Poisson point process $\mathcal{X}$, so the random sets J^λ and J^λ_ε are defined above, see (5.1), and then construct I^λ and I^λ_ε as functions of $\mathcal{X}$. Fix any $\lambda > 0$, and partition $\mathcal{X}^\varepsilon = \mathcal{X}^\varepsilon_\lambda$ into two sets: $\mathcal{X}^\varepsilon = \{x \in \mathcal{X}^\varepsilon : ||x|| > 1\} \cup \{x \in \mathcal{X}^\varepsilon : ||x|| < 1\} := \mathcal{X}^{\varepsilon,+} \cup \mathcal{X}^{\varepsilon,-}$. The points of $\mathcal{X}$ lying in $\mathcal{X}^{\varepsilon,+}$ and $\mathcal{X}^{\varepsilon,-}$ are $\mathcal{X}^{\varepsilon,+} = \{X_1, X_2, \ldots, X_{N'}\}$, $\mathcal{X}^{\varepsilon,-} = \{X_{N'+1}, \ldots, X_N\}$. Write $X_i = S_i\Theta_i$ for $i = 1, 2, \ldots, N'$, where $S_i > 1$ and $\Theta_i \in \mathbb{S}$, and set $C'_i = (S_i - 2)\Theta_i$ for $i = 1, 2, \ldots, N'$, while $C'_i = X_i$ for $i = N' + 1, \ldots, N$. Generate further points C'_i, $i = N + 1, \ldots, Z$, from a Poisson process of intensity λ in $\{x \in \mathbb{B} : ||x|| < 1 - \varepsilon\}$. Then we set $(I^\lambda)' = \bigcap_{i=1}^Z (C'_i + \mathbb{B})$ and $(I^\lambda_\varepsilon)' = \bigcap_{i=1}^N (C'_i + \mathbb{B})$. Note that the set $(I^\lambda_\varepsilon)'$ does not have exactly the same distribution as I^λ_ε: because $\text{Sh}^+(\varepsilon)$ has more volume than $\text{Sh}^-(\varepsilon)$, $(I^\lambda_\varepsilon)'$ has slightly more points than I^λ_ε. Also, since the shift map $s\theta \to (s-2)\theta$ is not an isometry, those points are no longer uniformly distributed over the inner shell. It remains to show that the error between these two point processes is small. The two distributions in question can be described as follows:

(i) I^λ_ε is formed by sampling a Poisson variable N with mean $\mu = \lambda\omega_d(1 - (1 - \varepsilon)^d)$ and placing N points on $\text{Sh}^-(\varepsilon)$ with i.i.d. uniform angles in $\mathbb{S}$ and i.i.d. radii R distributed as

$$\mathbb{P}(R \leq 1 - w) = H(w) = \frac{(1-w)^d - (1-\varepsilon)^d}{1 - (1-\varepsilon)^d}, \qquad w \in (0, \varepsilon).$$

(ii) $(I^\lambda_\varepsilon)'$ is formed by sampling a Poisson variable N' with mean $\mu' = \frac{\lambda}{2}\omega_d((1+\varepsilon)^d - (1-\varepsilon)^d)$ and placing N' points on $\text{Sh}^+(\varepsilon)$ with i.i.d. uniform angles in $\mathbb{S}$ and i.i.d. radii R' distributed as

$$\mathbb{P}(R' \leq 1 - w) = H'(w) = 1 - \frac{(1+w)^d - (1-w)^d}{(1+\varepsilon)^d - (1-\varepsilon)^d}, \qquad w \in (0, \varepsilon).$$

The difference between the means is $\mu' - \mu = \lambda\omega_d\left(\binom{d}{2}\varepsilon^2 + O(\varepsilon^3)\right) = O(\lambda\varepsilon^2)$.

By Proposition 4.1, $\text{TV}(N, N') \leq c\lambda\varepsilon^2$ for some $c > 0$. To couple the points of I^λ_ε and $(I^\lambda_\varepsilon)'$, first note that the random angles can be coupled directly, so it suffices to couple the radii. We

https://doi.org/10.1017/jpr.2021.34 Published online by Cambridge University Press

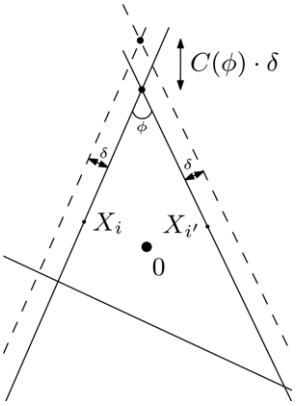


FIGURE 4. As long as the angles between intersecting hyperplanes are not too small, their d-fold intersections move by $O(\delta)$ if the hyperplanes are shifted by at most δ.

rely on an idea from optimal transport, namely the optimal coupling for the Wasserstein-1 distance, rather than total variation. The optimal coupling with respect to the L^1 distance is given by the transport map $H' \circ H^{-1}$: given R, the random variable $H'(H^{-1}(R))$ on the same probability space is distributed as R', and the average L^1 distance between R and R' is minimized for this coupling; see, for instance, [28, Section 2.1]. Explicit computations with series expansions show that, for $u \in (0, \varepsilon)$, $u - H' \circ H^{-1}(u) = O(\varepsilon^2)$. Since $\varepsilon^2 \ll \lambda^{-3/2}$ as $\lambda \to \infty$, for λ sufficiently large there exists a coupling between R and R' such that

$$|R - R'| \leq \lambda^{-3/2} \quad \text{almost surely as } \lambda \to \infty. \tag{5.2}$$

Let us summarize the proof up to this point, ignoring ε and λ for simplicity. We start with the points X_i close to $\partial\mathbb{B}$, which define the tessellation model J, a small set near the origin, whose boundary is composed of convex parts (corresponding to X_i lying just inside the unit ball $\mathbb{B}$) and concave parts (coming from X_i lying just outside $\mathbb{B}$). We then shift the X_i lying outside $\mathbb{B}$ to diametrically opposite points C_i'; this 'flips' the corresponding spheres, which are now centered at the C_i', so that the resulting set I' is now convex, being composed entirely of convex parts. This last step does not generate a random copy of I; we have introduced a slight distortion, in that the density of the points C_i' is not quite uniform. We thus have to shift the C_i' slightly in accordance with (5.2), so that the corresponding parts of the boundary of I' also shift a little, until we finally generate a truly random instance of the intersection model I.

Fact 4.1 and (5.2) together show that, in carrying out these two steps, the parts of the boundaries of the sets I and J corresponding to a fixed X_i are close (within Hausdorff distance $\lambda^{-3/2}$, before scaling). It remains to show that the sets I and J are themselves close. For this, we must exclude certain unlikely geometric configurations arising when different sphere boundaries intersect. Namely, if the angle at which some set of spheres meet is too small, shifting them by $\delta = \lambda^{-3/2}$ (as indicated in Fig. 4) could move the common intersection by much more than δ. See Fig. 4 for a diagram in dimension $d = 2$ (drawn with lines instead of circles for simplicity). To complete the proof, we need to show that the probability that these shifts move the boundary of J by more than $\lambda^{1/4}\delta = \lambda^{-5/4}$ tends to zero.

In dimension $d = 2$ (see Fig. 4), all we need to show is that each angle ϕ at each corner of the boundary of J is not too small. In higher dimensions, a slightly more complicated argument is

https://doi.org/10.1017/jpr.2021.34 Published online by Cambridge University Press

required; see below. We will use the fact that the points of J that move the most during shifting are the extreme points of J, so we focus attention on these extreme points, each of which is the common intersection of d bounding spheres.

By Fact 4.1, we may replace the spheres $X_i + \partial\mathbb{B}$ by hyperplanes $Y_i \cdot z = \alpha_i \varepsilon$, where $Y_i = (||X_i|| - 1) \cdot \frac{X_i}{||X_i||}$ and $0 < \alpha_i < 1$. To further simplify matters, we may upper bound the movement during shifting by assuming that all $\alpha_i = 1$, and that the total number of hyperplanes comprising the intersection is $O(\log^2 \lambda)$ (which holds with high probability, since the number of hyperplanes is Poisson with mean $C_d \log^2 \lambda$). Temporarily rescaling so that $||Y_i|| = \varepsilon = 1$, our task is to show that shifting any d of the hyperplanes $Y_{j_i} \cdot z = 1$ to $Y_{j_i} \cdot z = 1 + \delta$ moves their common intersection w (a single point) by no more than $O(\lambda^{1/4}\delta)$, with high probability. Equivalently, we need to show that w is not too large in modulus; specifically, we need $||w|| \leq C_d \lambda^{1/4}$, for some constant C_d depending only on d, with high probability.

Suppose not, so that $||w|| > C_d \lambda^{1/4}$, and recall that $Y_{j_i} \cdot w = 1$ for each $1 \leq i \leq d$. Choose w' parallel to w and in the affine span of the Y_{j_i}, so that $w' = \sum \beta_i Y_{j_i}$ with $\sum \beta_i = 1$. Then $||w'||||w|| = w' \cdot w = \sum \beta_i (Y_{j_i} \cdot w) = \sum \beta_i = 1$, so that $||w'|| < (C_d)^{-1} \lambda^{-1/4}$. In other words, the affine span of the Y_{j_i} passes within distance $(C_d)^{-1}\lambda^{-1/4}$ of the origin. For this to happen, some point Y_{j_d} lies within angular distance $C'_d \lambda^{-1/4}$ of a great hypersphere defined by some $d-1$ other points $Y_{j_1}, \ldots, Y_{j_{d-1}}$. There are $O(\log^{2(d-1)} \lambda)$ such choices for $Y_{j_1}, \ldots, Y_{j_{d-1}}$, and for a fixed such choice, the probability that Y_{j_d} lies within $\lambda^{-1/4}$ of their great hypersphere is $C''_d \lambda^{-1/4}$. Thus, each boundary intersection point is indeed not too large in modulus, and so does not move by more than $\lambda^{1/4}\delta = \lambda^{-5/4}$ after shifting, with high probability. Putting the pieces together, the sets I and J are within Hausdorff distance $\lambda^{-5/4}$ with high probability, and so $\mathbb{P}\big(d_{\mathrm{H}}(\lambda I^{\lambda}_{\varepsilon}, \lambda J^{\lambda}_{\varepsilon}) > C\lambda^{-1/4}\big) \to 0$, as desired. □

The final ingredient is a union bound.

Proof of Theorem 1.2. Combining Propositions 5.1 and 5.2 gives $\mathbb{P}(d_{\mathrm{H}}(\lambda J^{\lambda}, \lambda I^{\lambda}) > C\lambda\varepsilon^2) \leq \mathbb{P}(J^{\lambda}_{2\varepsilon} \neq J^{\lambda}) + \mathbb{P}(I^{\lambda}_{2\varepsilon} \neq I^{\lambda}) + \mathbb{P}(d_{\mathrm{H}}(\lambda J^{\lambda}_{2\varepsilon}, \lambda I^{\lambda}_{2\varepsilon}) > C\lambda^{-1/4}) \to 0$. □

This method could likely be applied to a wider class of intersection models: the ball $\mathbb{B}$ could be replaced by another set satisfying some curvature condition. The difficulty in such a generalization would lie in finding a canonical way to construct a coupling between the intersection model and another model known to have the Crofton cell of a tessellation model as a scaling limit.

6. The expected volume of I^{λ}

We first sketch Goudsmit's classical calculation for the second moment of the area A of a typical cell in a Poisson line tessellation T, when $d = 2$.

First, we recall some basic facts about T, which can be defined as follows. Let $\mathcal{P}$ be a unit-intensity Poisson process on $[0, 2\pi) \times \mathbb{R}^+$. We associate the point $(\theta, \rho) \in \mathcal{P}$ with the line $x \cos\theta + y \sin\theta = \rho$. This yields a translation- and rotation-invariant measure on families of lines in the plane; T is a random instance of this measure. It is not hard to show that the intersections of T and another random line form a Poisson process of rate 2, and also that T has π intersections, and thus π cells, per unit area.

Goudsmit [14] considered tessellations on the surface of a sphere, but we can rephrase his argument in terms of a realization of T over a large circular region R of area N. We choose two

https://doi.org/10.1017/jpr.2021.34 Published online by Cambridge University Press

points $x, y \in R$ uniformly at random and ask for the probability q_N that they lie in the same cell of T. If $f(t)$ denotes the density function for the area A of a typical cell, then, as $N \to \infty$,

$$Nq_N \to \frac{\int_0^\infty t^2 f(t)\,\mathrm{d}t}{\int_0^\infty tf(t)\,\mathrm{d}t} = \frac{\mathbb{E}(A^2)}{\mathbb{E}(A)},$$

since $tf(t)$ is the density function for the area of a cell containing a given point. On the other hand, x and y lie in the same cell of T if and only if the line segment l_{xy} joining them does not intersect T. As noted above, the number of intersections between l_{xy} and T is Poisson with rate 2, so there are no such intersections with probability e^{-2l}. Consequently, $Nq_N \to \int_0^\infty 2\pi l \mathrm{e}^{-2l}\,\mathrm{d}l = \frac{\pi}{2}$. Combining these two expressions yields the formula $\mathbb{E}(A^2) = \frac{\pi}{2}\mathbb{E}(A) = \frac{1}{2}$, which we may rewrite as

$$\frac{\mathbb{E}(A^2)}{\mathbb{E}(A)^2} = \frac{\pi^2}{2}.$$

Goudsmit's argument generalizes to higher dimensions. Write V_d for the volume of a typical cell in a Poisson hyperplane tessellation T_d in $\mathbb{R}^d$. This time we will choose a different normalization for the measure μ_{d-1} on the space $A(d, d-1)$ of affine hyperplanes in R^d, in which the measure of hyperplanes meeting the unit ball is 2, i.e. the diameter of the unit ball. Consequently, in the corresponding tessellation T_d, the expected number of hyperplanes H meeting the unit ball is two. With N now representing the volume of a large spherical region R, and q_N as before, we once again have

$$Nq_N \to \frac{\int_0^\infty t^2 f(t)\,\mathrm{d}t}{\int_0^\infty tf(t)\,\mathrm{d}t} = \frac{\mathbb{E}(V_d^2)}{\mathbb{E}(V_d)}$$

as $N \to \infty$. The second part of the calculation requires a slight modification; we now wish to estimate the number I_d of intersections of a line L of length l with T_d. Once again, I_d has a Poisson distribution, with mean c_d given by Crofton's formula [30, p. 172], namely

$$\frac{1}{l}\int_{A(d,d-1)} |L \cap H| \mu_{d-1}(\mathrm{d}H) = \frac{2\omega_{d-1}}{d\omega_d} := c_d,$$

where

$$\omega_d = \frac{\pi^{d/2}}{\Gamma(d/2+1)}$$

is the volume of the unit ball. Continuing the argument as before, and recalling that $S_d = d\omega_d$ is the surface area of the unit ball, we have

$$Nq_N \to \int_0^\infty S_d l^{d-1} \mathrm{e}^{-c_d l}\,\mathrm{d}l = \frac{d!}{c_d^d}\omega_d.$$

As before, this yields

$$\frac{\mathbb{E}(V_d^2)}{\mathbb{E}(V_d)} = \frac{d!}{c_d^d}\omega_d,$$

and, since (with this normalization) we have

$$\mathbb{E}(V_d) = \left(\frac{2}{c_d}\right)^d \frac{1}{\omega_d}$$

https://doi.org/10.1017/jpr.2021.34 Published online by Cambridge University Press

(see [21, pp.156, 179]), we conclude that

$$\frac{\mathbb{E}(V_d^2)}{\mathbb{E}(V_d)^2} = \frac{d!}{2^d}\omega_d^2,$$

in agreement with [21, p.179].

6.1. Intersection model

In this section we apply the above results to give an alternative proof of Proposition 1.1. This is essentially contained in Theorem 1.2 and the formulas above; Theorem 1.2 relates the volumes of I^λ and D_0^1, and the above analysis applies to D_0^1. The scaling in Theorem 1.2 relies on the scaling in Theorem 1.1, which was briefly sketched in the introduction. For completeness, we now explain the scaling in more detail, in the context of Theorem 1.2.

Suppose, then, that we know that the intersection $I^\lambda = I_d^\lambda$ converges to the Crofton cell of a suitably scaled Poisson hyperplane process, and we wish to determine the scaling.

First, consider the Poisson hyperplane model normalized, as above, so that the expected number of hyperplanes meeting the unit ball is two. Write $B_\varepsilon = \{x : ||x|| < \varepsilon\}$, so that the expected number of hyperplanes meeting B_ε is 2ε. For this process, the expected volume $\mathbb{E}(V_d^0)$ of the Crofton cell V_d^0 is related to the volume of the typical cell V_d as follows:

$$\mathbb{E}(V_d^0) = \frac{\mathbb{E}(V_d^2)}{\mathbb{E}(V_d)} = \frac{d!}{c_d^d}\omega_d = \frac{d!d^d\omega_d^{d+1}}{2^d\omega_{d-1}^d}.$$

The last two equalities come from the preceding section. The first equality is proved by calculating the probability that a point chosen uniformly at random in a large region lies in the same cell as the origin (as in the first part of Goudsmit's calculation).

Second, let us choose $\varepsilon = \varepsilon(\lambda) \to 0$ so that the expected number of spheres in the intersection model that meet B_ε tends to infinity. Then the intersection model inside B_ε is well-approximated by a Poisson hyperplane tessellation. The number of intersecting spheres meeting B_ε is the number of points of the underlying Poisson process in the shell $\mathrm{Sh}^-(\varepsilon) = \{x \in \mathbb{R}^d : ||x|| \in (1-\varepsilon, 1)\}$. This number is asymptotically $\varepsilon\lambda d\omega_d$, i.e. $\lambda d\omega_d/2$ times the 'normalized' value above. Consequently, as $\lambda \to \infty$,

$$\mathbb{E}(|I_d^\lambda|) = (1+o(1))\mathbb{E}(V_d^0)\left(\frac{2}{\lambda d\omega_d}\right)^d = (1+o(1))\frac{d!\omega_d}{\lambda^d\omega_{d-1}^d},$$

so that

$$\lim_{\lambda\to\infty} \lambda^d\mathbb{E}(|I_d^\lambda|) \to \frac{d!\omega_d}{\omega_{d-1}^d},$$

in agreement with Proposition 1.1.

7. Further questions

We close with some questions related to intersection processes that arose in the course of our research.

Question 7.1. *What class of intersection models has the Crofton cell of the hyperplane tessellation model D_0^1 as a scaling limit?*

https://doi.org/10.1017/jpr.2021.34 Published online by Cambridge University Press

Some kind of curvature condition is likely necessary. For example, consider the cone intersection model $I^{\rho,\lambda}_{\mathrm{Cone}(\vec{e}_1,\beta)}$ (discussed at the end of Section 3.2). Just like the hyperplane model, the cone model is a polyhedron. However, when $\beta \neq \frac{\pi}{2}$, each cone whose apex lies at the boundary of the intersection will contribute an additional vertex. Back-of-the-envelope calculations show that these vertices remain with positive probability in the limit $\lambda \to \infty$, which strongly suggests that the cone model does not have D^1_0 as a scaling limit.

Question 7.2. *Proposition 3.5 shows that the radius $R^{\mu,\lambda}_A$ converges to an exponential distribution under some rescaling. How does the rescaling relate to the geometry of A? How does it relate to the behavior of μ?*

For example, when $A = \mathbb{B}$, only the behavior of the density of μ near 0 matters in the limit.

Question 7.3. *Let S_λ denote the number of faces of the intersection model I^λ. Fact 4.2 suggests that S_λ is uniformly tight – i.e. that for any $\delta > 0$ there exists $t > 0$ such that for any $\lambda > 0$, $\mathbb{P}(S_\lambda > t) < \delta$ – which would imply the existence of a limiting stationary distribution for S. Can the limiting distribution and transition probabilities for the stochastic process $(S_\lambda)_{\lambda>0}$ be computed or approximated?*

A similar question has been answered for the typical Poisson–Voronoi cell and for the Crofton cell of a hyperplane tessellation, in a different limiting context [4,7]. The intersection construction of the Crofton cell D^1_0 seems ideal to study this question, because it has a natural renewal quality as λ increases.

Appendix A

In this appendix we recall the definition and some basic properties of Poisson point processes, which are used throughout this article.

Definition A.1. Let $\Omega \subset \mathbb{R}^d$ be a Borel set, and μ a finite Borel measure on Ω. The *Poisson point process* (PPP) on Ω with intensity μ, denoted $\mathcal{X}$, is the finite set consisting of $\mathrm{Poi}(\mu(\Omega))$-many independent points sampled from the probability measure $\frac{1}{\mu(\Omega)}\mu$.

This is a natural, intuitive definition; for a proper introduction to the theory of Poisson point processes, see [20].

Fact A.1. *Suppose $\mathcal{X}$ is a PPP on a Borel set $\Omega \subset \mathbb{R}^d$ with intensity meausre μ.*

(a) *Let $A \subset \Omega$ be any Borel set. Then $|A \cap \mathcal{X}| \sim \mathrm{Poi}(\mu(A))$.*

(b) *If $A, B \subset \Omega$ are disjoint Borel sets, then $\mathcal{X} \cap A$ and $\mathcal{X} \cap B$ are independent.*

An important special case of Fact A.1(a) is that the probability that a given region A contains no points of $\mathcal{X}$ is given by $\mathbb{P}(A \cap \mathcal{X} = \emptyset) = \exp(-\mu(A))$.

Appendix B

In this appendix we note a formula for finding the volume of a star-shaped domain in $\mathbb{R}^m$ by doing an integration over the $(m-1)$-dimensional sphere.

Fact B.1. *Suppose $g : \mathbb{S}^{m-1} \to \mathbb{R}^+$ is continuous, and let $A \subset \mathbb{R}^m$ be the star-shaped open set defined by $A = \{x \in \mathbb{R}^m : |x| < g(x/|x|)\}$. Then $\mathrm{Vol}(A) = \frac{1}{m}\int_{\mathbb{S}^{m-1}} g^m \, \mathrm{d}S$, where $\mathrm{d}S$ is the $(m-1)$-dimensional surface area form on $\mathbb{S}^{m-1}$.*

https://doi.org/10.1017/jpr.2021.34 Published online by Cambridge University Press

Proof. The formula comes from integrating in spherical coordinates. Applying Folland's theorem [10, Theorem 2.49] to the function $f(x) = 1\{x \in A\}$ gives

$$\begin{aligned}\mathrm{Vol}(A) &= \int_{\mathbb{R}^d} f(x)\,\mathrm{d}x \\ &= \int_{S^{m-1}} \int_0^{\infty} f(rx')r^{m-1}\,\mathrm{d}r\,\mathrm{d}\sigma(x') \\ &= \int_{S^{m-1}} \int_0^{g(x')} r^{m-1}\,\mathrm{d}r\,\mathrm{d}\sigma(x') \\ &= \frac{1}{m}\int_{S^{m-1}} g(x')^m\,\mathrm{d}\sigma(x').\end{aligned}$$

□

Acknowledgement

We wish to thank both referees for their very detailed comments.

Funding Information

Jacob Richey was supported by NSF grant DMS-1444084.

Competing Interests

There were no competing interests to declare which arose during the preparation or publication process of this article.

References

[1] ADELL, J. A. AND JODRÁ, P. (2006). Exact Kolmogorov and total variation distances between some familiar discrete distributions. *J. Inequal. Appl.* **2006**, 64307.
[2] BILLINGSLEY, P. (1995). *Probability and Measure*, 3rd edn. John Wiley, New York.
[3] BÖRÖCZKY, K. (2004). *Finite Packing and Covering*. Cambridge University Press.
[4] CALKA, P. (2003). An explicit expression for the distribution of the number of sides of the typical Poisson–Voronoi cell. *Adv. Appl. Prob.* **35**, 863–870.
[5] CALKA, P. (2019). Some classical problems in random geometry. In Stochastic Geometry, ed. D. COUPIER (Lect. Notes Math. 2237), Springer, Berlin, pp. 1–43.
[6] CALKA, P., MICHEL, J. AND PAROUX, K. (2009). Refined convergence for the Boolean model. *Adv. Appl. Prob.* **41**, 940–957.
[7] CALKA, P. AND SCHREIBER, T. (2005). Limit theorems for the typical Poisson–Voronoi cell and the Crofton cell with a large inradius. *Ann. Prob.* **33**, 1625–1642.
[8] CANNONE, C. (2017). A short note on Poisson tail bounds. Available at http://www.cs.columbia.edu/ccanonne/files/misc/2017-poissonconcentration.pdf.
[9] ERDÖS, P. AND RÉNYI, A. (1961). On a classical problem of probability theory. *Magyar Tudományos Akadémia Matematikai Kutató Intézetének Közleményei* **6**, 215–220.
[10] FOLLAND, G. B. (1999). *Real Analysis*. John Wiley, New York.
[11] FRANCESCHETTI, M. AND MEESTER, R. (2007). *Random Networks for Communication*. Cambridge University Press.
[12] GILBERT, E. (1961). Random plane networks. *J. Soc. Indust. Appl. Math.* **9**, 533–543.
[13] GILBERT, E. (1965). The probability of covering a sphere with N circular caps. *Biometrika* **56**, 323–330.
[14] GOUDSMIT, S. (1945). Random distribution of lines in a plane. *Rev. Mod. Phys.* **17**, 321–322.
[15] HALL, P. (1985). On the coverage of k-dimensional space by k-dimensional spheres. *Ann. Prob.* **13**, 991–1002.
[16] HALL, P. (1985). On continuum percolation. *Ann. Prob.* **13**, 1250–1266.
[17] HALL, P. (1988). *Introduction to the Theory of Coverage Processes*. John Wiley, New York.

https://doi.org/10.1017/jpr.2021.34 Published online by Cambridge University Press

[18] HAENGGI, M. (2013). *Stochastic Geometry for Wireless Networks*. Cambridge University Press.
[19] JANSON, S. (1986). Random coverings in several dimensions. *Acta Math.* **156**, 83–118.
[20] KINGMAN, J. F. C. (1992). *Poisson Processes*. Clarendon Press, Oxford.
[21] MATHERON, G. (1975). *Random Sets and Integral Geometry*. John Wiley, New York.
[22] MEESTER, R. AND ROY, R. (1996). *Continuum Percolation*. Cambridge University Press.
[23] MICHEL, J. AND PAROUX, K. (2003). Local convergence of the Boolean shell model towards the thick Poisson hyperplane process in the Euclidean space. *Adv. Appl. Prob.* **35**, 354–361.
[24] MILES, R. (1964). Random polygons determined by random lines in a plane I. Proc. Nat. Acad. Sci. USA 52, 901–907.
[25] MILES, R. (1964). Random polygons determined by random lines in a plane II. Proc. Nat. Acad. Sci. USA 52, 1157–1160.
[26] MOLCHANOV, I. (1996). A limit theorem for scaled vacancies of the Boolean model. *Stoch. Stoch. Rep.* **58**, 45–65.
[27] ROBBINS, H. E. (1944). On the measure of a random set. *Ann. Math. Statist.* **15**, 70–74.
[28] SANTAMBROGIO, F. (2015). *Optimal Transport for Applied Mathematicians*. Birkhauser, Basel.
[29] SANTALÓ, L. (1976). *Integral Geometry and Geometric Probability*. Addison Wesley, Boston.
[30] SCHNEIDER, R. AND WEIL, W. (2008). *Stochastic and Integral Geometry*. Springer, Berlin.

https://doi.org/10.1017/jpr.2021.34 Published online by Cambridge University Press